

# 9

## Future Prospects for High-energy Neutrino Astronomy

The history of neutrino physics and in particular high-energy neutrino astronomy at the South Pole depicts a success story over many decades. The major milestones along the path towards our current knowledge are illustrated in Figure 9.1. With the detection of atmospheric neutrinos in AMANDA in 2001 [183], and the discovery of astrophysical neutrinos in 2013 with the successor IceCube [2], both detectors achieved their primary objective shortly after their completion. Since then the IceCube collaboration confirmed this discovery in different distinct analyses. Yet no sources of these astrophysical neutrinos have been discovered within the first 10 years of detector lifetime. In 2018 the blazar TXS 0506+056 revealed first evidence for high-energy neutrino emission in multi-messenger studies (Section 4.4). As shown in the previous chapter such evidence could not be confirmed for the general case of blazar or any other source populations yet. Consequently, it seems reasonable to re-think the possible search strategies for the origin of high-energy astrophysical neutrinos. For this reason, we summarize the current status, potential, and issues of point source searches performed in IceCube in the first

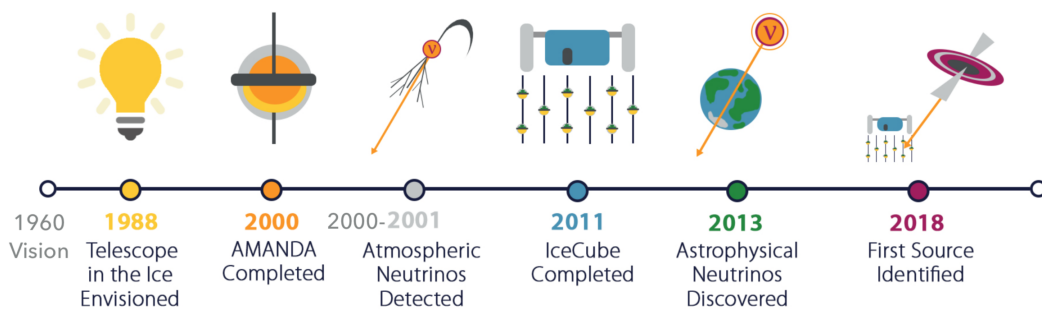


Figure 9.1: Timeline of the history of neutrino astronomy at the South Pole. The figure is taken from [182].

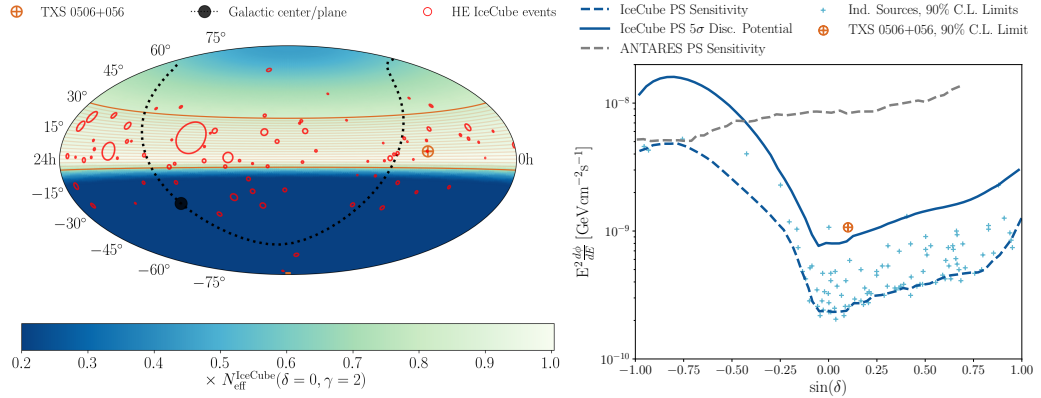


Figure 9.2: **Left:** Detection efficiency  $N_{\text{eff}}$  of the IceCube detector. The orange band indicates the most optimal region for neutrino point source searches with this setup. **Right:** Sensitivity and  $5\sigma$  discovery potential for neutrino point sources with 10 years of IceCube data. The data are taken from [3].

section of this chapter. Afterward, we propose a global neutrino telescope network of existing and prospective neutrino observatories and study its potential in Section 9.2.

## 9.1 Current Status of High-energy Neutrino Point Source Searches

Since the first discovery of an astrophysical neutrino flux in 2013, the IceCube collaboration has raised large efforts to localize the origin of these events. Next to independent searches within neutrino data, several known astrophysical objects and populations (e.g. the 3FHL blazar population in Chapter 8) have been studied for their neutrino emission. While one of these multi-messenger studies revealed evidence for neutrino emission from the blazar TXS 0506+056, no source has been discovered at a  $5\sigma$  level within the first 10 years of detector lifetime. In order to develop further strategies of neutrino point source searches, the status and the potential of current analyses with IceCube is illustrated in both panels of Figure 9.2. The sky map in the left panel illustrates the detection efficiency  $N_{\text{eff}}$  of the IceCube detector defined as

$$N_{\text{eff}}(\delta, \gamma) = \int_0^\infty A_{\text{eff}}(\delta, E_{\nu_\mu}) E_{\nu_\mu}^{-\gamma} dE_{\nu_\mu}, \quad (9.1)$$

for a source with spectral index  $\gamma = 2$ . In general, the detection efficiency is proportional to the number of expected astrophysical events  $N_{\nu_\mu}$  (Equation (7.27)) from a source

with spectral index  $\gamma$ . The distribution in the left panel of Figure 9.2 nicely shows that for sources with hard  $\gamma = 2$  power-law spectra, the detection efficiency rapidly drops in the Southern Hemisphere below  $\delta \sim -5^\circ$ . This effect is caused by atmospheric muons vastly dominating the event rate in this region. Above  $\delta = 30^\circ$  the detection efficiency of the IceCube observatory also drops in the Northern Hemisphere due to the absorption of high-energy neutrinos inside the core of the Earth. Hence the optimal region of the IceCube detector for such sources is limited to the region around the horizon from approximately  $-5^\circ$  to  $30^\circ$ . Although IceCube constantly observes neutrinos from every direction in the Universe, this means that only  $\sim 30\%$  of the sky is covered with optimal sensitivity. The distribution of high-energy track-like events, most likely representing astrophysical muon neutrino events clarify this observation. The vast majority of these events are located in the region around the horizon. Some high-energy events are also detected in the Southern Hemisphere by means of vetoing techniques, that only yield minor enhancements for statistical searches of neutrino point sources. Two more points are worth to be noted from the illustration of this sky map. Firstly, the blazar TXS 0506+056 is located exactly within the optimal region of the IceCube detector and thus has an maximal probability to be detected. Secondly, we can see that only a small part of the galactic plane is covered by the region around the horizon, while a large part including the galactic center can only be studied with the considerably worse sensitivity in the Southern Hemisphere.

The distribution of the sensitivity and discovery potential sources with a  $\gamma = 2$  spectrum, shown in the right panel of Figure 9.2 reassures the improved sensitivity of IceCube at the horizon for hard sources. Besides it also provides additional information about the potential of future neutrino point source discoveries. Next to the sensitivity and discovery potential of IceCube<sup>1</sup>, the flux limits of several potentially interesting sources are shown (blazars, etc.). Several of these sources reveal limits close to the one observed for TXS 0506+056 and in particular close to the flux threshold required for discovery. Hence it might be possible that we just reached the threshold for many more neutrino sources similar to TXS 0506+056. Improving the performance of the current analyses might shed light on this speculation. The fundamental question is, if such improvements can be realized by means of additional data from the IceCube detector. In order to answer this question we have to contemplate the temporal evolution of the sensitivity and discovery potential with increasing amount of data. We can identify theoretical boundaries by considering two extreme scenarios. Assuming that the region around the hypothetical source is dominated by background, then the statistical

---

<sup>1</sup>Note that both thresholds are not corrected for the look elsewhere effect that arises from scanning the whole sky.

fluctuations of these background events evolve with the square root of the total amount of events<sup>2</sup> and hence the measuring time  $t$ . The amount of the signal events on the other hand increases linearly with  $t$  (Equation (7.27)), yielding an improvement of the discrimination between signal and background that is proportional to

$$\frac{d\phi_{\text{thr}}^{\min}}{dE_\nu}(t, t_0) \propto \frac{1}{\sqrt{t/t_0}}, \quad (9.2)$$

where  $\frac{d\phi_{\text{thr}}}{dE_\nu}$  can be both, the flux threshold for the sensitivity as well as the discovery potential and  $t_0$  depicts an artificial reference time. In a background free environment, the improvement of the analyses performance only depends on the linear growth of the signal event rate, yielding

$$\frac{d\phi_{\text{thr}}^{\max}}{dE_\nu}(t, t_0) \propto \frac{1}{t/t_0}. \quad (9.3)$$

The actual evolution of the discovery potential for single point source searches as well as for population searches such as the 3FHL blazar stacking in Chapter 8 depict an average of both scenarios [158]. Assuming a single power-law with spectral index  $\gamma = 2$ , the performance for both analyses improves with

$$\frac{d\phi_{\text{thr}}}{dE_\nu}(t, t_0) \propto \sim \frac{1}{(t/t_0)^{0.8}}. \quad (9.4)$$

This means that the performance of point source analyses can be improved by  $\sim 40\%$  when doubling the amount of experimental data. Hence additional data represent a powerful tool to improve the sensitivity of point source analyses throughout the first years of data-taking. Nevertheless current point source analyses in IceCube already make use of  $\sim 10$  years of data. Hence significant improvements in the performance of the analyses can not be expected from the collection of more data<sup>3</sup>.

In 2014 the IceCube collaboration proposed an extension of the current IceCube detector, called *IceCube-Gen2* [184]. This successor is supposed to instrument  $10 \text{ km}^3$  of glacial ice, with the spacing of the modules optimized for high-energy muon neutrino tracks. Due to the potential improvements of the reconstructions (a long lever arm allows both, improved directional as well as energy reconstructions) and a vast increase in statistics, this detector aims to improve the performance of point source analyses by a factor of  $\sim 5$  with respect to the current IceCube detector. While *IceCube-Gen2* could

---

<sup>2</sup>Similar to the standard deviation of a poissonian distribution.

<sup>3</sup>Note that neutrino flares could by chance still yield discoveries of neutrino sources with the current setup.

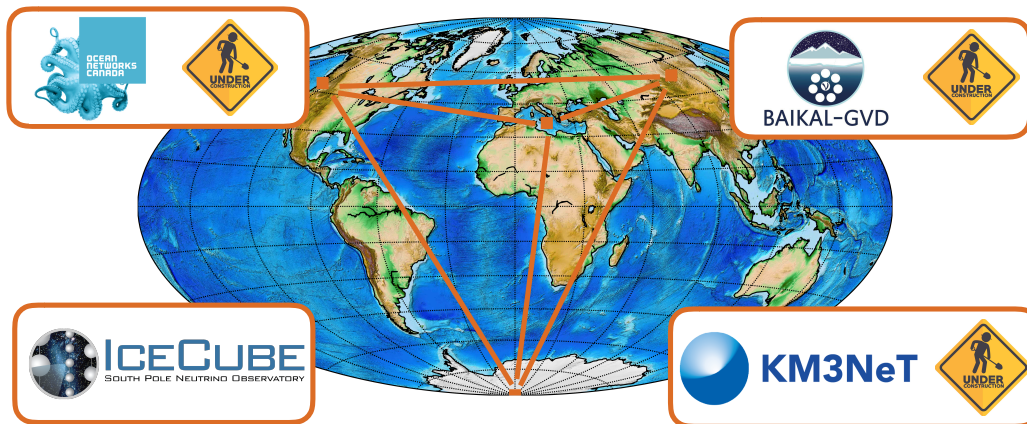


Figure 9.3: Location of the observatory sites of the available large volume neutrino telescopes.

overcome the flux threshold to discover neutrino sources at the horizon, its optimal performance is limited to the region around the horizon, hence missing roughly 70 % of the entire sky<sup>4</sup>.

## 9.2 Prospects towards a Global Neutrino Telescope Network

Despite being the only neutrino telescope build in ice, IceCube is not the only neutrino observatory on our planet that aims to detect high-energy neutrinos. With the Baikal Gigaton Volume Detector (Baikal-GVD)[135], the Cubic Kilometer Neutrino Telescope (KM3NeT)[133] and the Pacific-Ocean Neutrino Explorer (P-ONE)[185] three more neutrino detectors based in water are under construction or running in partially finished configurations (Subsection 6.4.2). All of these neutrino observatories attempt to find the origin of high-energy astrophysical neutrinos, bringing light into the physics involved in multi-messenger astronomy. The different sites of these observatories are marked on the world map shown in Figure 9.3.

In order to improve the sensitivity for a discovery of high-energy neutrino sources, we investigate the combined performance of a global network of all four neutrino telescopes. We will call this global network *Planetary Neutrino Monitoring system* (PLE $\nu$ M) throughout this thesis [185]. Using a combined effort of all existing resources

---

<sup>4</sup>Note that both IceCube and IceCube-Gen2 are actually observing these parts in the sky as well but only with limited sensitivity.

will not only offer maximal sensitivity towards the detection of neutrino sources but can also solve the challenges obtained by the individual detectors (such as for instance the declination dependent analysis performance in IceCube). In the following chapter, we will study the potential of PLE $\nu$ M. In a first step, we compare the optimal field of views from the respective detection site before we derive estimates for the sensitivity and discovery potential of the global telescope network based on simplified, yet conservative detector assumptions.

### 9.2.1 Combined Field Of View of PLE $\nu$ M

As mentioned repeatedly throughout this thesis, the performance of point source analysis in IceCube is optimal for sources located at the horizon. In this region, the event rate is neither dominated by atmospheric muons (because of the shielding of the Earth) nor affected strongly by the absorption of the high-energy part of the neutrino flux in the Earth's core. These effects are not the result of any specific detector geometry but are solely caused by the particular location of the detection site. Hence we expect a similar behavior for each of the other telescopes as well. Yet, instead of the actual horizon, their best field of view will be at the respective detector *horizon* of their observation site. A combined field of view of all four neutrino telescopes is shown in Figure 9.4, assuming that the optimal detection range of each telescope is similar to the one from IceCube from  $\delta \in \{-5^\circ, 30^\circ\}$ .

Although being an extremely simplified consideration, this illustration already provides valuable information about the behavior and the potential of a combined telescope network. While IceCube's performance constantly peaks at the horizon, the optimal detection regions of the other telescopes shift throughout one day due to the rotation of the Earth. These shifts are illustrated by the four panels in Figure 9.4, which are respectively shifted by 6 h (corresponds to  $90^\circ$ ). From each of these skymaps, it is obviously visible that a large region of the Universe is covered by at least one of the telescopes in optimal configuration at any point in time. Based on the optimal angular observation range chosen for this illustration roughly 85 % of the sky are provided with optimal exposure of PLE $\nu$ M. The missing fraction mostly resides in the region close to the North Pole, which is not covered by any of the telescopes.

Despite the extension of the total exposure of the Universe by nearly a factor of 3, the potential of PLE $\nu$ M compared to IceCube can be highlighted by means of two specific examples. As previously mentioned, a large fraction of the galactic plane including the galactic center is located in the low-performance region of the IceCube detector. Using a combined telescope network completely changes this picture. As visible in Figure 9.4

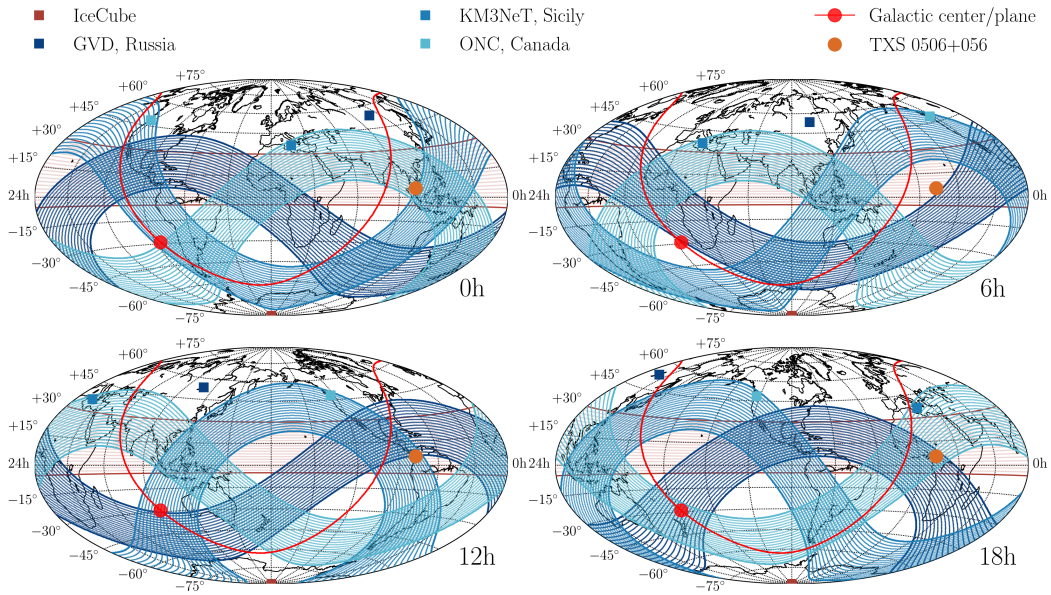


Figure 9.4: Optimal field of views from different detection sites at different observation times. While IceCube is not affected by the rotation of the Earth due to its exceptional location, the optimal field of views of the Universe from the other telescope sites are shifted with time.

the galactic center, as well as a large fraction of the galactic plane, constantly appear within the optimal detector performance region of one of the observatories. In this way, not only the time-integrated flux but even short transient emission of sources from this region could be observed. Note that in principle this improvement is not restricted to galactic phenomena, but could be applied to any kind of neutrino source that is not located close to the North Pole.

Next to the study of galactic phenomena, a combined neutrino telescope network could be also used to strengthen or rule out the discovery of neutrino sources for instance at the horizon. This can be exemplary demonstrated by looking at the particular example of the blazar TXS 0506+056, that showed evidence for neutrino emission at a  $3.5\sigma$  level within IceCube data between September 2014 and March 2015 [5]. From Figure 9.4, it becomes clear that in the case of TXS 0506+056 being a source, a roughly similar neutrino signal should have been visible in a combined effort of the remaining three telescopes. Observing a signal at a similar level ( $3.5\sigma$ ) would boost the individual IceCube result to a combined outcome of PLE $\nu$ M very close to a point source discovery at  $\sim 4.8\sigma^5$ . In a similar way, the signal observation by IceCube could have been

---

<sup>5</sup>Based on Fisher's method for two independent results bearing upon the same null hypothesis [186].

sanctioned and potentially ruled out by not detecting any signal by any of the other telescopes.

### 9.2.2 Neutrino Point Source Discovery Potential of PLE $\nu$ M

In the previous subsection, we pointed out the potential of PLE $\nu$ M that arises from the superposition of the best field of views from the individual telescopes. Nevertheless, in this simplified view, we completely neglect that each of these observatories also observes neutrinos outside these regions with lower sensitivity towards point source searches. In this subsection, we want to include the full potential of each telescope in order to derive a realistic estimation of the sensitivity and discovery potential of a combined network. Since none of the telescopes apart from IceCube reached their final detector configuration yet, we cannot rely on performance measurements from these sites. In order to estimate the combined potential of PLE $\nu$ M anyway, we built our study on the basic detector assumptions from IceCube. In the following, we will assume that each of the neutrino telescopes included in PLE $\nu$ M performs exactly like the IceCube detector, but at its respective telescope location. Since each of the new telescopes under construction (KM3NeT, Baikal-GVD and P-ONE) are designed to outperform IceCube in the search for high-energy neutrino sources, this depicts a very conservative assumption. Consequently also the values for the discovery potential that will be shown depict conservative estimates, that will most likely be outperformed by the actual implementation of PLE $\nu$ M.

Since all of the telescopes within the network of PLE $\nu$ M can be treated as independent observatories, we can use a linear superposition of the individual effective areas

$$A_{\text{eff}}^{\text{PLE}\nu\text{M}} = \sum_k A_{\text{eff}}^k, \quad (9.5)$$

with  $k \in \{\text{IceCube}, \text{KM3NeT}, \text{Baikal-GVD}, \text{P-ONE}\}$ . On the basis two essential facts we can use this effective area to evaluate the combined potential. Initially we recall from Equation (7.27), that the number of observable events from a steady emitting source with flux  $\frac{d^2\phi_{\nu_\mu}}{dt dE}$  is defined as

$$N_{\nu_\mu} = \int_{\Delta E} A_{\text{eff}}(E, \delta) \frac{d^2\phi_{\nu_\mu}}{dt dE} dE \tau, \quad (9.6)$$

where  $\tau$  depicts the total observation time. Similar to the total observation time  $\tau$ , the effective area  $A_{\text{eff}}$  incorporates linearly in this definition. Hence constant changes in

either of the two parameters have similar effects on the number of signal events. In this sense we observe twice the amount of signal events  $N_{\nu_\mu}$  from doubling the effective area as well as from doubling the total observation time. In the beginning of this chapter we have observed that the performance quantities such as the sensitivity and the discovery potential evolve with  $\tau^{-0.8}$  (Equation (9.4)) for point source analyses in IceCube. For the performance study in this section we will attribute changes of the effective area to relative changes in the observation time. The observation time  $\tau$  that the IceCube detector needs to observe the similar amount of events as PLE $\nu$ M within  $\tau_0$  is

$$\tau = \tau_0 \frac{\int_{\Delta E} A_{\text{eff}}^{\text{PLE}\nu\text{M}}(E, \delta) \frac{d^2\phi_{\nu_\mu}}{dtdE} dE}{\int_{\Delta E} A_{\text{eff}}^{\text{IceCube}}(E, \delta) \frac{d^2\phi_{\nu_\mu}}{dtdE} dE}. \quad (9.7)$$

In this sense, the PLE $\nu$ M network can be interpreted as extension of IceCube's observation time by a factor of  $\tau/\tau_0$ . Ultimately using the time evolution monitored in IceCube allows an approximate evaluation of the sensitivity and discovery potential of PLE $\nu$ M.

Using the approximated effective areas, based on the assumption that detectors are similar to IceCube we can evaluate these performance magnitudes for the PLE $\nu$ M network. The effective area depends on both declination and energy. Hence on grounds of better manageability, we make use of the detection efficiency  $N_{\text{eff}}$  instead. Assuming a source following a single power-law distribution, both parameters are correlated according to Equation (9.1). The detection efficiencies of all four telescopes for one specific but artificial moment in time are shown in Figure 9.5. Similar to IceCube, the performance of the other telescopes is best at their respective horizon and drops vastly towards their respective southern hemisphere that is dominated by atmospheric muons. While the rotation of the Earth hardly affects neutrino studies for IceCube<sup>6</sup>, the local detection efficiency of the other telescopes rapidly changes throughout one day. Since we are mostly interested in time-integrated neutrino emission studies over many months up to years, we only care for the detection efficiency averaged over time periods larger than a few days. These average detection efficiencies with respect to IceCube are shown in Figure 9.6. Note that due to very similar latitude (or declination) of the observation sites of KM3NeT, Baikal-GVD and P-ONE their average detection efficiencies are very similar.

In order to generate the scenario of PLE $\nu$ M, we can simply take the sum of the average detection efficiencies of the individual observatories<sup>7</sup>. By comparing this sum

---

<sup>6</sup>Note that this only counts for analysis that search for neutrino emission in time windows that are larger than a few days.

<sup>7</sup>For sources following a single power-law this shows a similar effect as the superposition of the effective areas (Equation (9.5)).

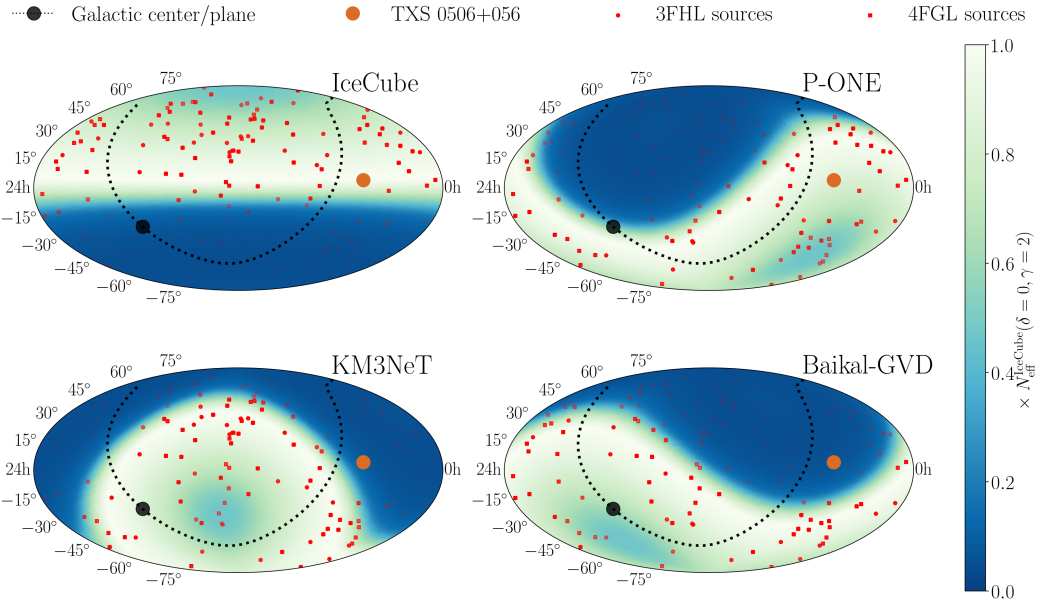


Figure 9.5: Detection efficiency for a source following a single power-law spectrum with  $\gamma = 2$  at one artificial moment in time for all neutrino telescopes that are part of the PLE $\nu$ M performance study. The respectively 100 sources with the highest gamma-ray emission within the 3FHL and the 4FGL catalog are illustrated as well [165, 187].

to the respective values for IceCube yields estimates for the increase in observation time  $\tau/\tau_0$ . In the following we will use three different expressions for the resulting sensitivity and discovery potential values. Next to the absolute values  $\frac{d\phi_{\text{thr}}^{\text{conf}}}{dE_\nu}$  for these performance parameters, we also show the improvement of the detector configuration compared to IceCube at its optimal location  $\delta = 0$  defined as

$$R_0(\delta, \gamma) := \frac{d\phi_{\text{thr}}^{\text{IceCube}}}{dE_\nu}(\delta = 0, \gamma) / \frac{d\phi_{\text{thr}}^{\text{conf}}}{dE_\nu}(\delta, \gamma), \quad (9.8)$$

and the relative improvement at the actual location defined as

$$R_{\text{rel}}(\delta, \gamma) := \frac{d\phi_{\text{thr}}^{\text{IceCube}}}{dE_\nu}(\delta, \gamma) / \frac{d\phi_{\text{thr}}^{\text{conf}}}{dE_\nu}(\delta, \gamma). \quad (9.9)$$

The improvements of PLE $\nu$ M compared to IceCube for similar observation times and sources with unbroken power-law  $\gamma = 2$  is shown in Figure 9.7. The skymap in the left panel directly reveals that PLE $\nu$ M opens a window to basically every point in the Universe with at least the optimal sensitivity of IceCube at the horizon. Even in the

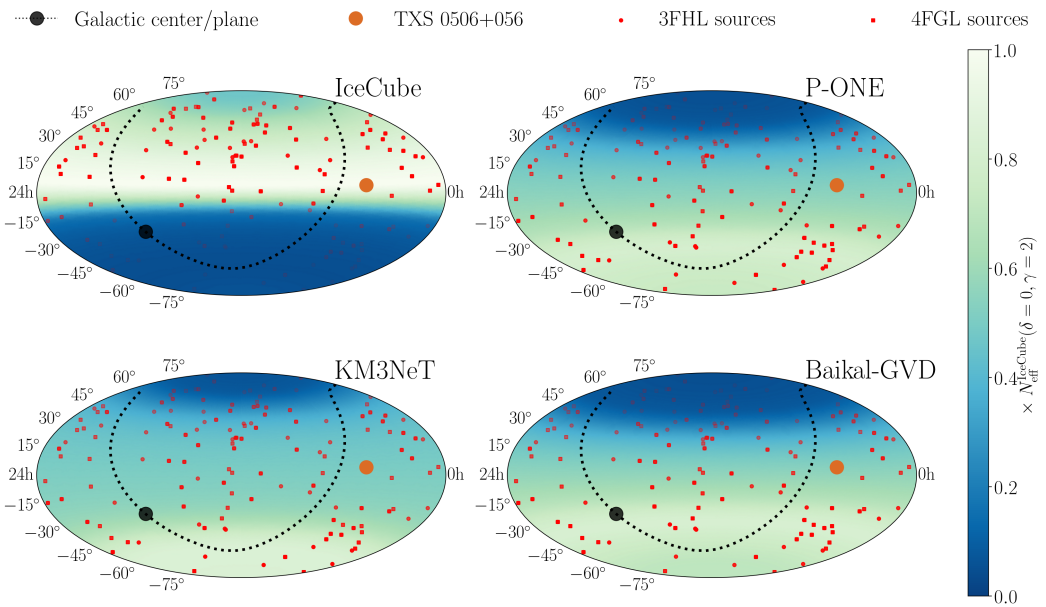


Figure 9.6: Detection efficiency for a source following a single power-law spectrum with  $\gamma = 2$  averaged over time periods of  $> 1$  d for all neutrino telescopes that are part of the PLE $\nu$ M performance study. The respectively 100 sources with the highest gamma-ray emission within the 3FHL and the 4FGL catalog are illustrated as well [165, 187].

region close to the North Pole approximately 75 % of IceCube’s optimal performance are reached. Hence a global neutrino telescope network could accomplish a complete survey of the sky for these kinds of neutrino sources. Comparing the explicit performance at each declination directly reveals that PLE $\nu$ M improves the point source analysis performance by more than a factor of 20 in the Southern Hemisphere and at least a factor of 2 everywhere else.

The spectral shape of potential neutrino sources is still unknown. In fact, while for instance, most theoretical models for blazars predict spectral shapes harder than the general assumption of  $\gamma = 2$ , the IceCube measurements reveal that the spectral shape of the entity of astrophysical neutrinos most likely follows a power-law distribution with a softer spectral index. In order to study both scenarios in the context of PLE $\nu$ M, similar comparisons as shown in Figure 9.7 for  $\gamma = 2$ , are shown in Figure 9.8 for sources with  $\gamma = 1.5$  and  $\gamma = 2.5$  respectively. Similar to the scenario for  $\gamma = 2$  neutrino sources, the skymaps in the left panels illustrate that by means of PLE $\nu$ M nearly the whole Universe can be studied with at least the optimal sensitivity of IceCube at the horizon. The explicit improvements at the respective declinations  $R_{\text{rel}}$  are differing for

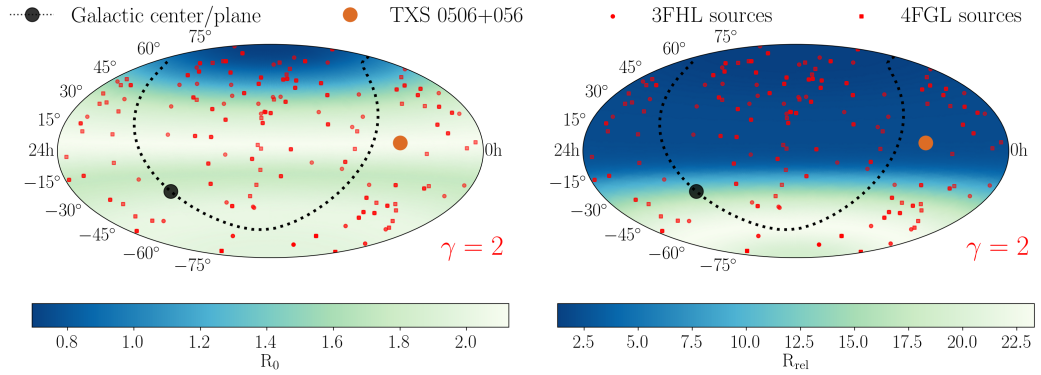


Figure 9.7: Performance of PLE $\nu$ M with respect to IceCube for similar run times and sources following an unbroken power-law distribution with spectral index  $\gamma = 2$ . The respectively 100 sources with the highest gamma-ray emission within the 3FHL and the 4FGL catalog are illustrated as well [165, 187].

the two scenarios. For sources with a hard spectral index of  $\gamma = 1.5$ , IceCube performs best at the horizon. Nevertheless also the sensitivity in the Southern Hemisphere enhances compared to softer sources because the on average higher energies of the neutrino events offer a better discrimination power with respect to low-energy atmospheric muons. Consequently the explicit improvement  $R_{\text{rel}}$  (top right panel of Figure 9.8) in the Southern Hemisphere is less than for softer sources, yet still achieves a factor of  $\sim 5$ . While the relative performance of IceCube in the Southern Hemisphere increases for hard sources, the absorption of high-energy neutrinos in the core of the Earth yields a decline in the region close to the North Pole. Hence the combined telescope network will also yield improvements by a factor  $\sim 5$  for sources with  $\gamma = 1.5$ . For sources following a softer power-law distribution of  $\gamma = 2.5$  the situation is exactly the other way round. In the region above the horizon, PLE $\nu$ M will outperform IceCube by more than a factor of  $\sim 2.5$ . In the Southern Hemisphere, IceCube's sensitivity for neutrino point sources drops drastically for soft sources. This is caused by the poor energy discrimination between atmospheric muons and neutrinos and low-energy astrophysical neutrinos. The remaining telescopes in the PLE $\nu$ M framework can compensate IceCube's weak performance, yielding improvements of more than a factor of 160 in this region.

Up to now we always showed comparisons of PLE $\nu$ M and IceCube based on the assumption that both instruments measure over the same time period. Nonetheless, the IceCube collaboration already measured neutrino data by means of its full detector configuration for more than 10 years. In order to display a more realistic scenario for the PLE $\nu$ M network, we want to account for this fact. In the following, we will investigate

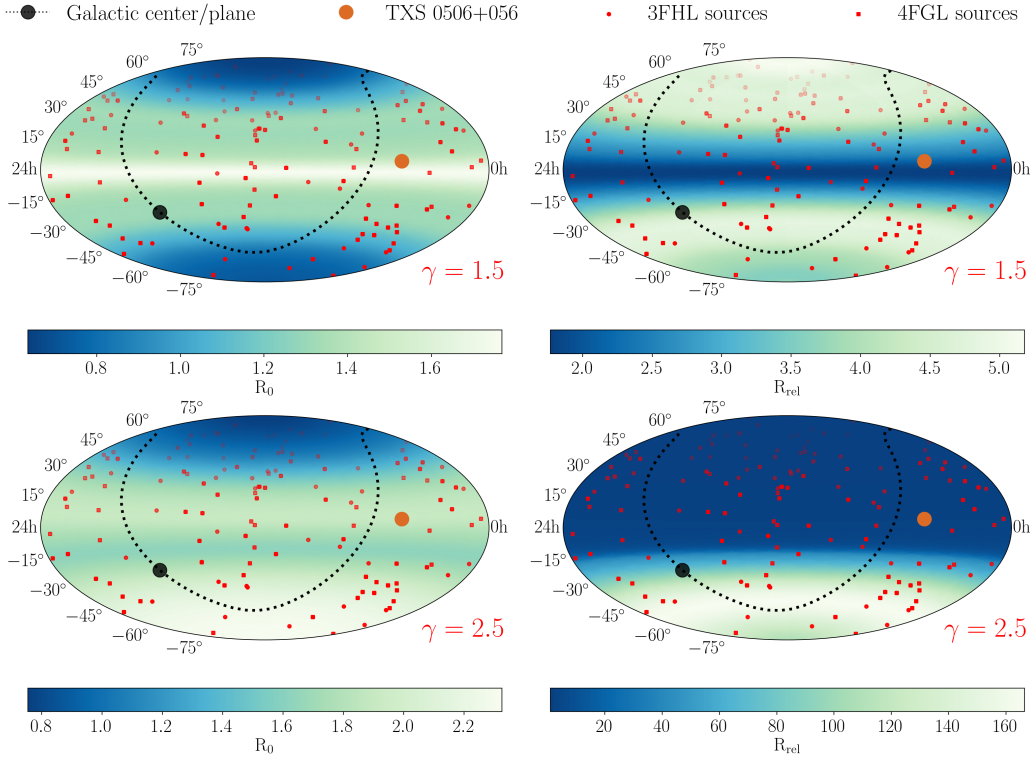


Figure 9.8: Performance of PLE $\nu$ M with respect to IceCube for similar run times and sources following an unbroken power-law distribution with spectral index  $\gamma = 1.5$  and  $\gamma = 2.5$ . The respectively 100 sources with the highest gamma-ray emission within the 3FHL and the 4FGL catalog are illustrated as well [165, 187].

the improvements of PLE $\nu$ M, if we turn on this global network after 10 years of exclusive runtime of IceCube. The evolution of the relative improvements  $R_{\text{rel}}$  with increasing lifetime for sources following a power-law distribution with  $\gamma = 2$  is illustrated in Figure 9.9. We can see that even after the first year of PLE $\nu$ M the sensitivity towards point sources improves by a factor of four in the Southern Hemisphere. After three years the performance in the south already enhances by a factor of  $\sim 8$  evolving to a factor of  $\sim 14$  after 10 years. At the horizon PLE $\nu$ M enhances the sensitivity by  $\sim 50\%$  after 5 years and  $\sim 70\%$  after 10 years.

### 9.2.3 PLE $\nu$ M and IceCube Gen-2

As previously mentioned at the beginning of this chapter, not only new neutrino telescopes are under construction but also the IceCube collaboration itself plans a high-

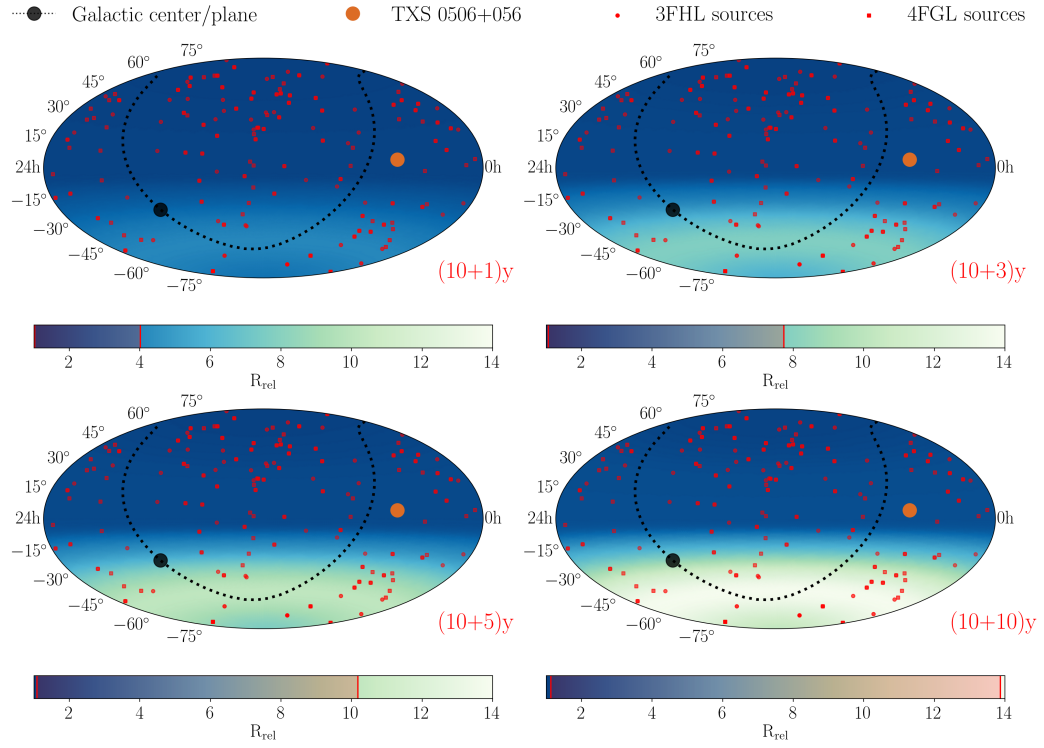


Figure 9.9: Relative improvements due to  $(x)$ yr of PLE $\nu$ M compared to IceCube running for  $(10 + x)$ yr. The red band in the colorbar indicates the range of the values apparent in the respective skymap. The respectively 100 sources with the highest gamma-ray emission within the 3FHL and the 4FGL catalog are illustrated as well [165, 187].

energy extension, called IceCube Gen-2, around the currently existing detector volume that could yield a gain for point source sensitivities by a factor of  $\sim 5$ . In the following, we will include this successor in the scenario of PLE $\nu$ M. In the left panel of Figure 9.10 the relative improvement  $R_{\text{rel}}$  of a global neutrino telescope network including IceCube Gen-2 compared to IceCube is shown for sources following a power-law with  $\gamma = 2$ . Similar to before we presume for this study that IceCube already measured data for 10 years before PLE $\nu$ M and the IceCube upgrade start their operation for additional 10 years. Similar to the before the largest improvement compared to IceCube arises in the Southern Hemisphere. Yet, as a result of the IceCube upgrade Gen-2 also the performance at the horizon and in the Northern Hemisphere increases by nearly a factor of 4.

In the right panel of Figure 9.10 the influence of KM3NeT, Baikal-GVD, and P-ONE

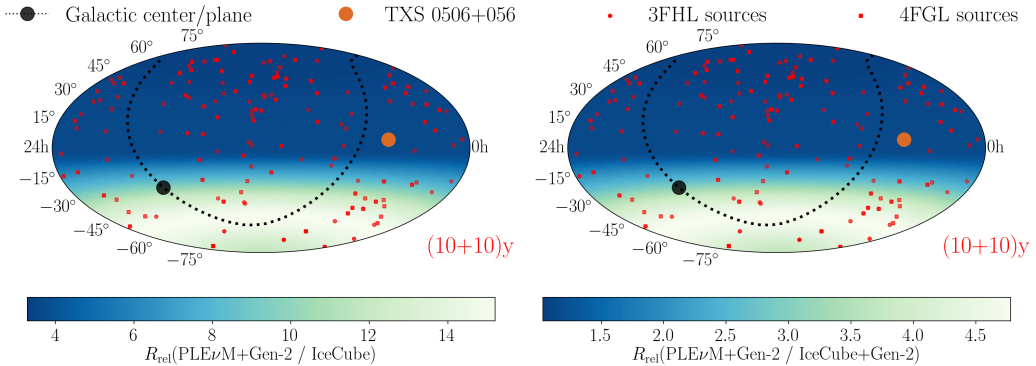


Figure 9.10: **Left:** Relative improvements for sources with spectral index  $\gamma = 2$  due to additional 10 yr of PLE $\nu$ M and Gen-2 compared to IceCube running for 20 yr. **Right:** Relative improvements due to additional 10 yr of PLE $\nu$ M and Gen-2 compared to IceCube and Gen-2 running for (10 + 10) yr respectively. The respectively 100 sources with the highest gamma-ray emission within the 3FHL and the 4FGL catalog are illustrated as well [165, 187].

within this scenario is illustrated. Including these detectors to IceCube and IceCube-Gen2 yields large improvements to sensitivity in the Southern Hemisphere. Nevertheless in the Northern Hemisphere and at the horizon IceCube Gen-2 dominates the sensitivity in this scenario. Note that this specific outcome is strongly affected by the primary assumption made in this study, which established that all other telescopes (except IceCube Gen-2) operate similar to the IceCube detector. In fact, since probably all of these detectors will outperform IceCube in terms of point source sensitivities, all results shown in this study can be interpreted as conservative estimates.

Ultimately the absolute values for the  $5\sigma$  discovery potential for the previous scenario are shown in Figure 9.11. As visible, the discovery potential of the combined network of PLE $\nu$ M+Gen2 would cover the 90 % C.L. upper limits for all tested sources from [3]. In order to reach the discovery potential of the combined network of PLE $\nu$ M and IceCube Gen-2 at the horizon and the Northern Hemisphere after 10 years of runtime, IceCube would need to observe the sky for additional  $\sim 100$  years. To accomplish a similar performance in the Southern Hemisphere, IceCube would need to run for auxiliary  $\sim 350$  years.

### 9.3 Conclusion

The study described in this chapter revealed that a combined network of neutrino telescopes at different detection sites can vastly improve the point source sensitivity of

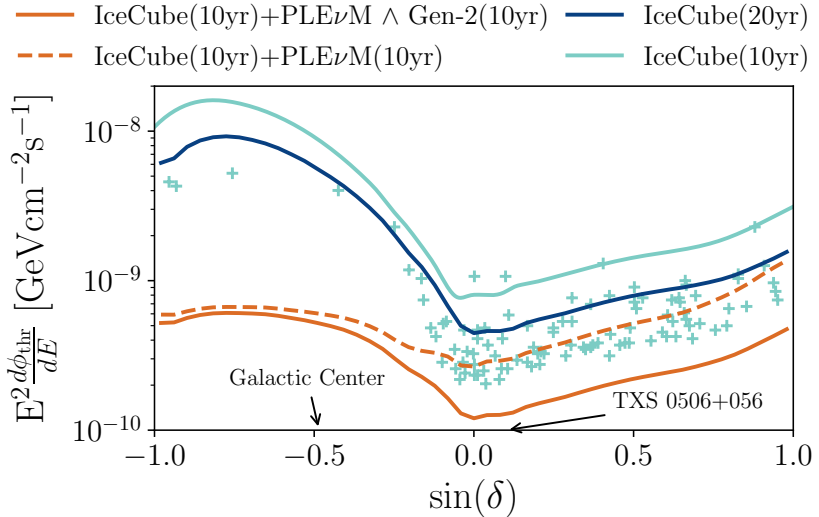


Figure 9.11:  $5\sigma$  discovery potential of different telescope networks. The markers indicate the current limits for interesting objects tested by IceCube [3]. The location of the galactic center and TXS 0506+056 are indicated by the black arrows.

IceCube within a few years. While a large factor of this enhancement at the horizon and in the Northern hemisphere can be attributed to the IceCube upgrade Gen-2, the Southern Hemisphere can only be accessed by means of the other telescopes. In order to optimally access the region close to the North Pole, another neutrino telescope located somewhere in the Southern Hemisphere would be necessary.

The study in this chapter only consider point source searches based on track-like events mainly induced by muons and muon neutrinos. In ice, these track-like events allow for a median angular resolution of less than  $1^\circ$  at energies above 1 TeV. Hence they depict the optimal event type to observe the local clustering of neutrinos from astrophysical sources. In contrast, due to scattering and their spherical appearance, cascade-like events from electron neutrinos and NC interactions can only be reconstructed with a median accuracy of  $10^\circ$  to  $15^\circ$  in IceCube (Subsection 6.4.1). As a consequence cascade-like events in ice are barely valuable in the search of their sources.

This situation changes for neutrino telescopes in water. In water, the propagation of Cherenkov light is mainly dictated by absorption effects, while scattering only depicts a minor influence. Hence, depending on the spacing of the detector modules, more direct un-scattered photons can be observed which subsequently yields the chance for enhanced reconstructions. The median angular resolution for track-like events in KM3NeT is roughly  $0.2^\circ$  above 10 TeV, while cascade-like events above 100 TeV can

still be reconstructed with a median angular uncertainty of  $1.5^\circ$  [188]. In this scenario, not only track-like events but also the second major event topology can be used for the study of neutrino point sources. While track-like events still outperform the directional reconstruction of cascade-like events, the latter appears to obtain other major advantages for point source searches. In contrast to track-like events, the energy of observable cascade-like events is mostly contained inside detector volume, allowing for an accurate energy reconstruction. The accurate knowledge of their energy can be utilized to discriminate against the atmospheric background. Moreover, the total event rate of cascade-like events at higher energies is not influenced by atmospheric muons that dominate the rate of track-like events. Hence their total rate is mainly constituted by atmospheric and astrophysical neutrino events. In combination with the accurate energy estimation, cascade-like events in water-based neutrino telescopes can introduce a second alternative facility to discover astrophysical neutrino sources. The exact potential of these events in this context requires a detailed dedicated study for the respective telescope.